Si and Ge nanocluster formation in Silica matrix

© Roushdey Salh, L. Fitting×, E.V. Kolesnikova+, A.A. Sitnikova+,
M.V. Zamoryanskaya+, B. Schmidt*, H.-J. Fitting

Institute of Physics, University of Rostock,
D-18051 Rostock, Germany
× School of Applied and Engineering Physics, Cornell University,
Ithaca 14853 N.Y., USA
+ Ioffe Physicotechnical Institute, Russian Academy of Sciences,
194021 St. Petersburg, Russia
* Research Center Rossendorf, Institute of Ion Beam Physics and Materials Research,
01310 Dresden, Germany

(Получена 12 сентября 2006 г. Принята к печати 3 октября 2006 г.)

High resolution transmission electron microscopy, scanning transmission electron microscopy and cathodoluminescence have been used to investigate Si and Ge cluster formation in amorphous silicon dioxide layers. Commonly, cathodoluminescence emission spectra of pure SiO_2 are identified with particular defect centers within the atomic network of silica including the nonbridging oxygen hole center associated with the red luminescence at 650 nm (1.9 eV) and the oxygen deficient centers with the blue (460 nm; 2.7 eV) and ultraviolet band (295 nm; 4.2 eV). In Ge^+ ion implanted SiO_2 an additional violet emission band appears at 410 nm (3.1 eV). The strong increase of this violet luminescence after thermal annealing is associated with formation of low-dimension Ge aggregates like dimers, trimers and higher formations, further growing to Ge nanoclusters. On the other hand, pure silica layers were modified by heavy electron beam irradiation (5 keV; 2.7 A/cm^2) leading to electronic as well as thermal dissociation of oxygen and appearance of under-stoichiometric SiO_x. This SiO_x will undergo a phase separation and we observe Si cluster formation with a most probable cluster diameter of 4 nm. Such largely extended Si clusters will diminish the SiO_2 related luminescence and Si crystal related luminescence in the near IR appears.

PACS: 61.46.Df, 61.72.Tt, 61.82.Fk, 78.60.Hk

1. Introduction

Amorphous silicon dioxide (α-SiO_2) is an important dielectric material with diverse use in modern microelectronic devices [1] and optical fiber communications [2,3]. Irradiation of SiO_2 induces various types of structural defects and acts as direct source for nanocluster formation within the silica matrix, on the other hand, high quality modified silica-based materials are highly required in the speedy developed Si electronic technology, especially those related to thin oxidized layers.

The physical properties of small nanometer-sized particles have received considerable attention in recent years, driven by both fundamental and technological interests. The optical properties of semiconductor crystalline or amorphous nanoclusters embedded in insulating matrices have been of particular interest in this regard. Such structures are usually prepared by ion implantation which is a commonly used technique for the addition of dopants to thin layers and can effortlessly produce nanometer-sized clusters within the host material. Thus ion implantation offers possibilities of local concentrations higher than that obtainable by other methods, as well as the fact that almost any element can be introduced. The optical properties of the glass, such as absorption [4], photoluminescence [5], and nonlinear optical properties [6], are significantly affected by the presence of dopants and nanoclusters. Hence silicon and germanium are common dopants in silica technology. Ge implantation is frequently used in a variety of applications in communication and sensing technology such as photoinduced Bragg gratings in optical fibers. In this way Ge atoms can be located in the SiO_2 host network and, probably, give rise to the cathodoluminescence emission at 3.1 and 4.2 eV, see [7,8].

In this article, we focus on the use of cathodoluminescence spectroscopy in combination with energy-dispersive X-ray analysis hosted both in a scanning electron microscope to understand the physical structure and formation mechanisms of Si and Ge nanoclusters and their influence on the luminescence defect centers. Moreover, the formation of Si and Ge nanoclusters in the amorphous silica matrix is demonstrated by high-resolution transmission electron microscopy (HR-TEM) and scanning transmission electron microscopy (STEM).

2. Experimental set-up

The cathodoluminescence (CL) measurements were performed in a digital scanning electron microscope (Zeiss DSM 960). The CL spectra over the wavelength 200–800 nm were detected via a parabolic mirror collector and analyzed with a Spex-270M spectrograph then registered by a charge coupled device (CCD) camera in single shot technique at short time of 1 s and with a spectral resolution of 4 nm. A cooling and heating temperature stage changed the sample temperatures between 80 and 670 K. In general, the CL excitation was performed

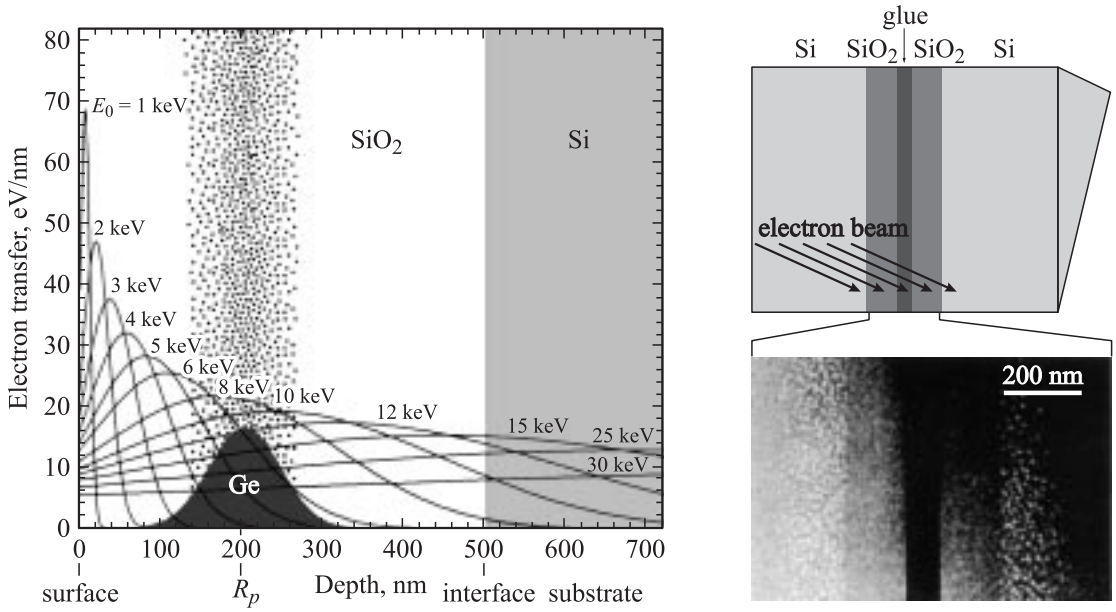

Figure 1. Electron beam excitation densities in SiO_2 layers for different beam energies E_0. Here we show the Ge^+ implantation profile in the mean projected range $R_p = 200$ nm. On the right hand side a STEM micrograph of the sample is shown in cross section technique.

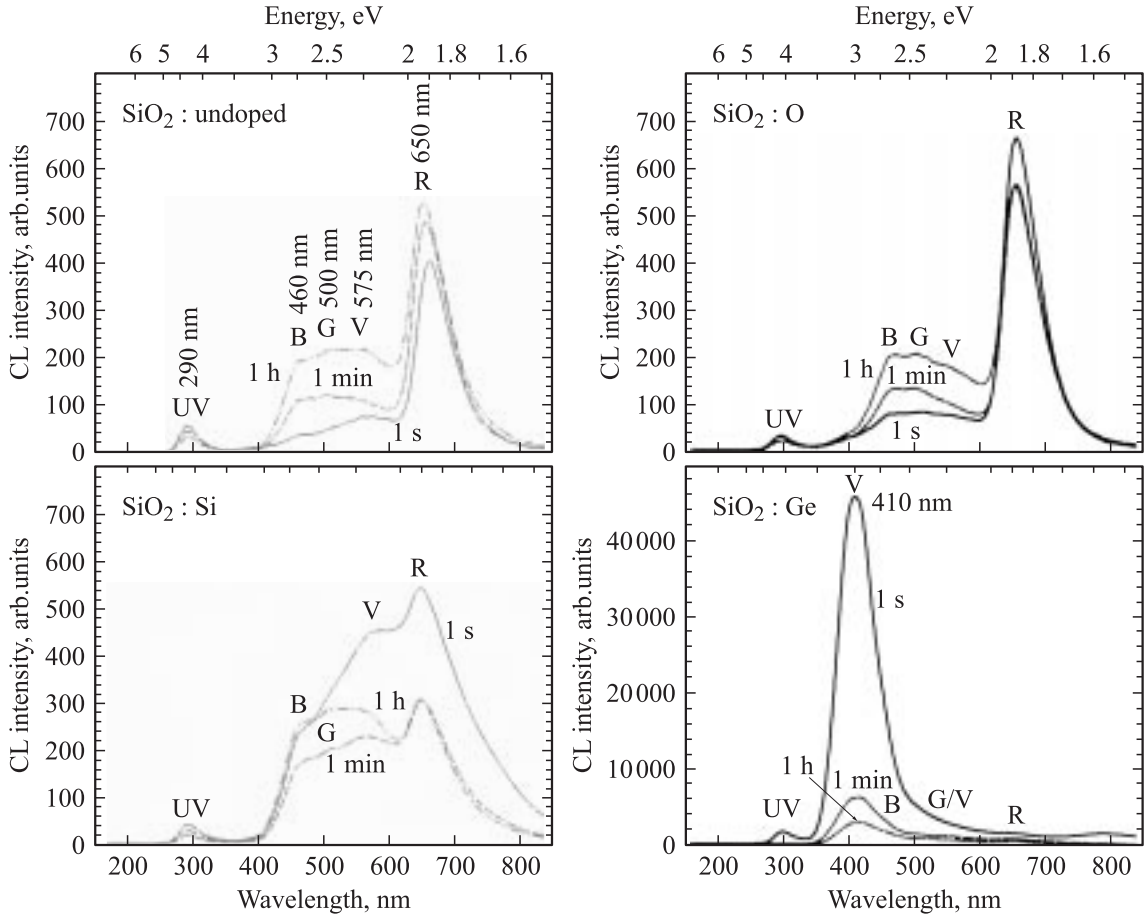

Figure 2. Typical CL-spectra of a pure SiO_2 layer in comparison to O^+, Si^+ and Ge^+ implanted layers recorded at room temperature. Note the huge violet (V) band in SiO_2:Ge; all after a post-implantation thermal annealing at $T_a = 900°C$.

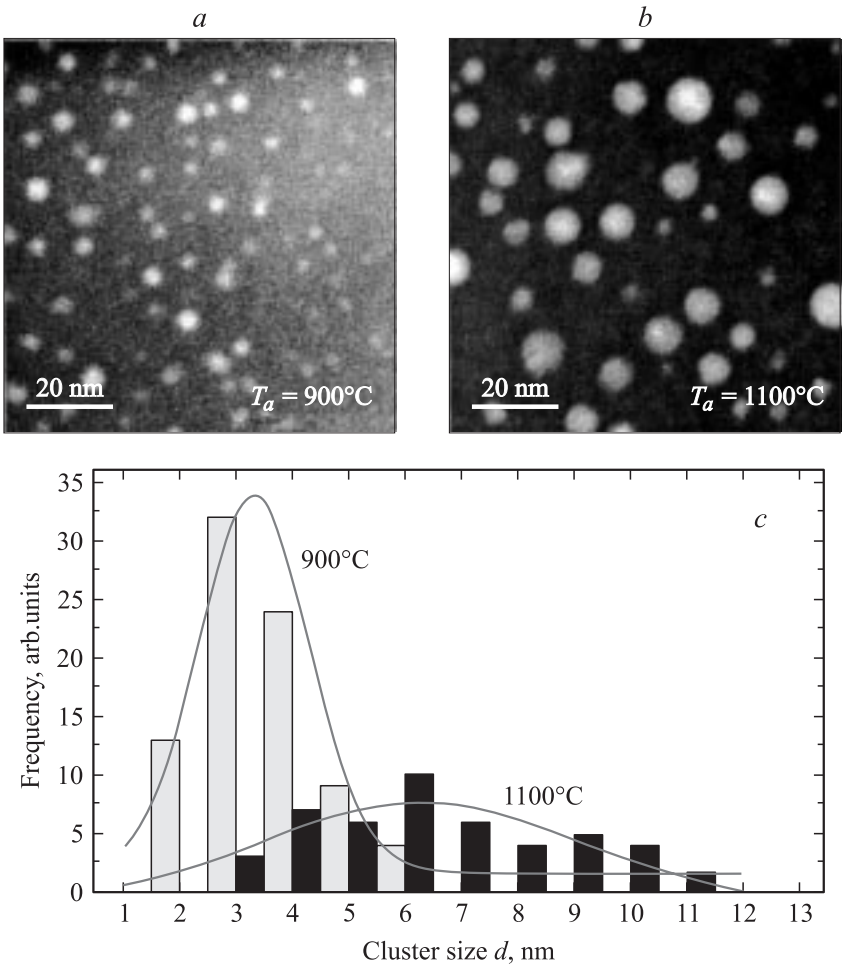

Figure 3. STEM cross section images of Ge implanted SiO_2 layers showing clusters growing by Ostwald ripening (a, b) with increasing annealing temperatures T_a, as well as the respective Ge cluster diameter distributions (c). The correlated cluster concentrations: a — $N_c = 4.6 \cdot 10^{17}\,\mathrm{cm}^{-3}$ for $T_a = 900^\circ\mathrm{C}$, and b — $N_c = 2.6 \cdot 10^{17}\,\mathrm{cm}^{-3}$ for $T_a = 1100^\circ\mathrm{C}$.

with electron energies of 2–30 keV and beam currents of about 100 nA in TV scanning mode over an area of $2.9 \cdot 10^{-5}\,\mathrm{cm}^2$. This corresponds to an electron beam current density $j_0 \approx 3.3\,\mathrm{mA/cm}^2$. With 512×512 pixels the scanning beam focus of a diameter $\sim 1\,\mu$m is strongly ($\sim 90\%$) overlapping from pixel to pixel and guarantees a homogeneous excitation over the excited area.

As samples we have used amorphous, thermally grown SiO_2 layers, 500 nm thick, wet oxidized at 1100°C on a Si substrate. The layers are of microelectronic quality. Their mass density is $2.26–2.29\,\mathrm{g/cm}^3$. Several layers have been doped by ion implantation with Ge^+ ions of an energy of 350 keV, with Si^+ ions of 150 keV, and O^+ ions of 100 keV, all with a uniform dose of $5 \cdot 10^{16}$ ions/cm^2 leading to an atomic dopant fraction of about 4 at% roughly at the half depth of the SiO_2 layer, i. e. at a depth of the mean projected ion range of about 250 nm. The full width of the half maximum of the implanted profiles is about 130 nm, see Fig. 1.

The dopant profiles have been calculated by the Monte Carlo simulation program TRIM [9]. The implantation was performed by an ion beam of a diameter ~ 1 cm in scanning mode over an area of $7 \times 7\,\mathrm{cm}^2$. Thus the scanning imhomogenity was less than 5%. During implantation the sample temperature was kept below 80°C. Afterwards, a post-implantation thermal anneal was performed at temperature $T_a = 900$ and 1100°C for 1 h in dry nitrogen for the germanium implanted samples and in vacuum for both the oxygen and silicon implanted samples. The growth of Si and Ge nanoclusters has been shown by means of a scanning transmission electron microscope STEM (200 keV FEI Tecnai F20) in cross section technique as demonstrated in Fig. 1 (right). Si nanoclusters have been made visible by transmission electron microscopy (100 keV TEM, EM-420 Philips).

3. Results and Discussion

The main luminescent centers in pure and ion implanted silica are the red luminescence $\lambda \approx 650$ nm (1.9 eV) of nonbridging oxygen hole center (NBOHC) and the oxygen

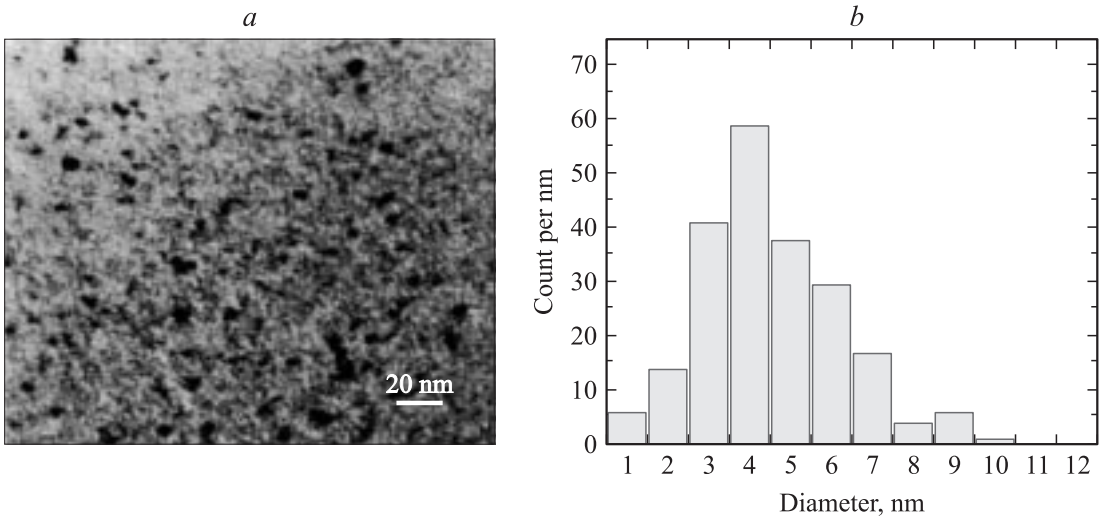

Figure 4. TEM micrograph showing Si nanoclusters embedded in the silica matrix (a) and the related cluster size distribution (b) in a 250 nm SiO_2 layer having been irradiated for 30 min by an electron beam of 5 keV and current density 2.7 A/cm^2.

deficient centers (ODC) with a blue (B) $\lambda \approx 460$ nm (2.7 eV) and ultraviolet (UV) luminescence $\lambda \approx 290$ nm (4.2 eV), as to be seen in Fig. 2 where the spectra of pure SiO_2 layers on a Si substrate as well as doped with Ge^+, Si^+, and O^+ ions are compared. In Ge-doped amorphous SiO_2 layers an additional luminescence band is detected at $\lambda \approx 410$ nm (3.1 eV) and the red luminescence from the NBOHC center of the SiO_2 matrix is conserved. The larger amplitude of the violet band (V) at $\lambda \approx 410$ nm (3.1 eV) seems to be overtaken from the tetragonal GeO_2 (rutile) modification indicating a strong defect luminescence at the Ge dopant centers in the rutile coordination [7,10].

However, the main investigation in the present paper is aimed to the direct comparison of the stoichiometric SiO_2 layer and the Si^+, and Ge^+ implanted SiO_2 layers in Fig. 2 in context with the blue band (B) at $\lambda = 460$ nm and red band (R) at $\lambda = 650$ nm intensities. In Fig. 2 we recognize a larger blue (B) emissivity of the Si^+ implanted layer compared to the pure and the O^+ implanted ones as well as a larger red (R) luminescence of the O^+ implanted samples with respect to the Si^+ inplanted ones. Thus we state that a silicon surplus or, in other words, oxygen deficiency in SiO_2 increases the blue luminescence, whereas an oxygen surplus does not affect the blue luminescence but increases the red luminescence. Obviously, the oxygen deficient centers as origin of the blue luminescence as well as the nonbridging oxygen for the source of the red luminescence are consistent with these data.

In Ge^+ implanted samples, the red band appears also in the detection range but is not as dominant as in the standard SiO_2 spectra. In a previous work [7] we have demonstrated that the spectra of Ge doped amorphous SiO_2 layers are a mixture of SiO_2 and tetragonal GeO_2. The violet luminescence is related to different states or phases of Ge, namely to GeO_2 dissolved in the near SiO_2 surface region and to Ge nanoclusters [11] located deeper in the SiO_2 layers which may be partially oxidized at their interface to the surrounding amorphous SiO_2 matrix. The nanocluster size is growing with annealing temperature from 2–4 nm at $T_a = 900$°C to 5–10 nm at $T_a = 1100$°C as shown in Fig. 3.

The formation of oxygen deficient centers or even higher silicon aggregates by means of electron beam irradiation has been manifested already earlier, see e.g. [7,12,13]. Even Auger electron spectroscopy has clearly evidenced that oxygen is dissociated from SiO_2 due to electronic or thermal processes during electron beam excitation, see e.g. [14]. Thus the blue and the red luminescence bands are growing under electron bombardment to a saturation after an irradiation dose of about 3 A/cm^2, see [7].

In order to demonstrate the oxygen dissociation and the formation of ODC, and finally, of Si clusters under electron bombardment, we have carried out an additional experiment under high dose electron irradiation. Therefore thin 250 nm-thick silica films have been prepared by wet thermal oxidation on silicon wafers. Afterwards the silicon substrate had been removed by mechanical polishing and 3 keV Ar^+ ion etching. In this way self-supporting 250 nm thin silica films had been prepared for imaging in a transmission electron microscope. More details of preparation are given in [15]. These films were modified by heavy electron beam irradiation: beam energy 5 keV, current 20 nA over an area of $3/4\,\mu$m^2 yielding in a high current density of 2.7 A/cm^2. Thus we may assume electronic as well as thermal dissociation [16] of oxygen from the thin SiO_2 layers and more and more the appearance of under-stoichiometric SiO_x. This SiO_x will undergo a phase separation described as below:

$$SiO_x \rightarrow \frac{x}{2}SiO_2 + \left(1 - \frac{x}{2}\right)Si, \quad 1 < x < 2. \qquad (1)$$

After 30 min electron beam irradiation we observe Si cluster formation as presented in Fig. 4. The Si clusters

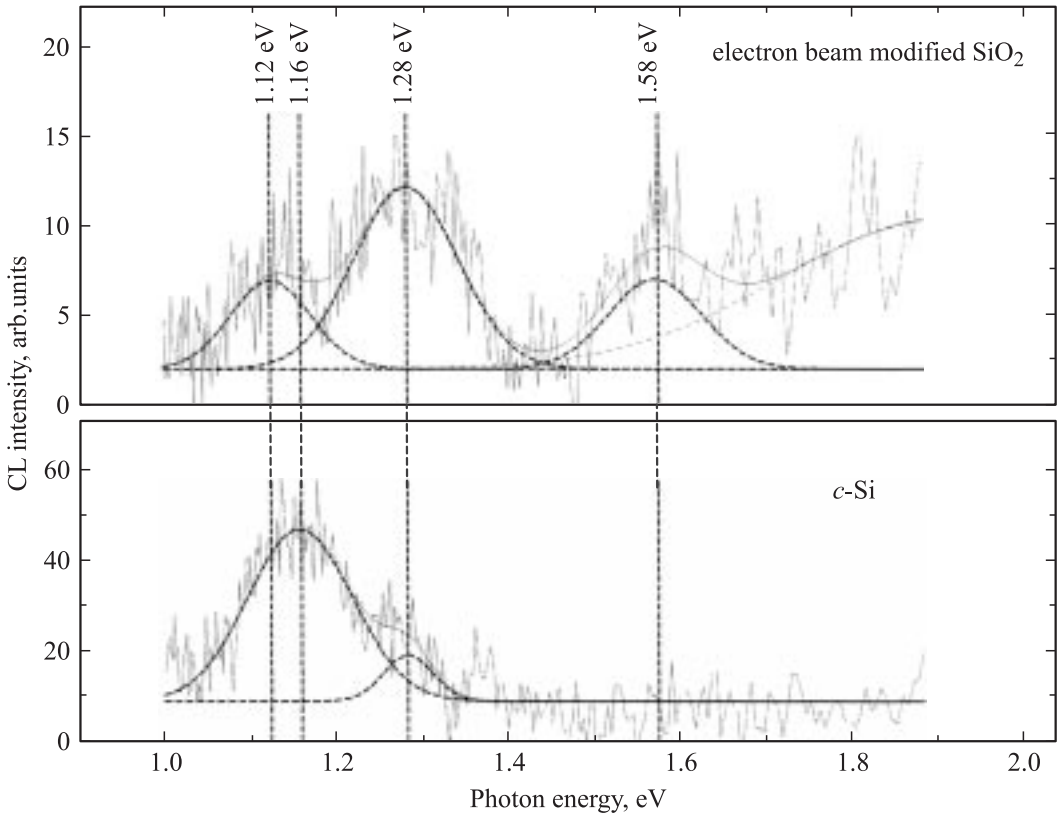

Figure 5. CL spectra of electron beam modified SiO_2 showing in the near IR fundamental transition of *c*-Si at $h\nu = 1.1$ eV, of *a*-Si at 1.3 eV and a probable transition in Si nanocrystals (quantum dots) at 1.6 eV.

embedded in the silica appear as dark sports. Their size distribution is shown in the right part of Fig. 4. There we see a most probable cluster diameter of 4 nm and a maximum diameter of 10 nm. As we have already shown in context with formation of Ge nanocrystallites in Ge-implanted silica [7], such largely extended clusters will diminish the Si related luminescence. The right size for elementary small luminescent clusters should be searched in intermediate regions, i. e. between Si dimers (ODC) and hexamer rings [17,18].

Fig. 5 shows the CL spectra of pure crystalline Si and the spectra of Si (*c*-Si) nanoclusters embedded in the host silica. Luminescence bands are observed at around 1.1 and 1.3 eV assigned to crystalline and amorphous silicon (*c*-Si) phases, respectively. Another band at 1.6 eV is also to be seen after heavy electron beam bombardment in the SiO_2 structure. In spite of extensive experimental and theoretical work during the last years, the light-emitting mechanism which explains emission at 1.6 eV has not been fully understood yet. It is believed that the oxygen-related light-emitting centers are positioned at the interface between the Si nanoclusters and the host oxide [19]. A broad CL emission band is characteristic of Si nanoclusters. Although the spectra vary considerably in intensity after longer irradiation, the peak position is not significantly shifting, implying a similar mean size for the nanocrystals. No unique relation between the CL or PL emission energies and Si nanocluster sizes has been reported in the literature making the quantitative comparison of the results difficult [20]. Other authors estimated that 5 nm Si nanoclusters emit at 1.6 eV, while 3 nm Si nanoclusters give PL at 2 eV [21]. On the contrary it was reported that 4 nm Si nanoclusters emit at 1.3 eV and the 1.6 eV PL correspond to very small sizes of about 1 nm [22].

Recently Si nanocrystals have been fabricated by thermal treatment of $SiO-SiO_2$ nanolattices, in a way which enables to control not only the size but also the density and the arrangements of the nanocrystals [23,24]. In this method a strong photoluminescence (PL) and a size dependent shift of the PL position are shown as a proof for size control. A strong blue shift from 960 nm (1.3 eV) to 810 nm (1.5 eV) with decreasing nanocrystals size was observed with respective cluster sizes 3.8 nm and 2 nm, respectively.

4. Conclusion

Electron irradiation of amorphous layers *a*-SiO_2 induces chemical defect reactions dependent on the sample oxidation, thermal annealing and temperature. The red band R (1.9 eV; 650 nm) in CL spectra is associated with the non-bridging oxygen hole center (NBOHC) whereas the blue band B (2.7 eV; 460 nm) and the ultraviolet band UV (4.2 eV; 295 nm) are attrubuted to the Si related oxygen

deficient center (SiODC). In Ge^+-implanted SiO_2 a huge violet band V (3.1 eV; 410 nm) associated with the Ge related oxygen deficient center (GeODC) dominates the CL spectra. After thermal annealing in dry nitrogen or in vacuum at temperature around $T_a = 900°C$ all luminescence bands grow. Thus the SiODC's as well as the GeODC's are formed by Si and Ge molecules clustering to dimers, trimers and higher aggregates. With further aggregation and growth to Si and Ge nanocrystals embedded in the SiO_2 matrix, the blue and the violet ODC luminescence decreases again. The nanoclusters size are growing with annealing temperature from 2–4 nm at $T_a = 900°C$ to 5–10 nm at $T_a = 1100°C$. Further on, heavy electron beam bombardment of SiO_2 and associated oxygen dissociation creates Si nanoclusters in the size range of 2–10 nm with a most probable diameter of 4 nm giving rise to the luminescence in the near IR at 1.3 and 1.6 eV.

References

[1] E.H. Nicollian, J.R. Brews. *MOS* (*Metal Oxide Semiconductor*) *Physics and Technology* (Wiley, N.Y., 1982).
[2] I. Fanderlik. *Silica Glass and it's Application* (Elsevier, 1991).
[3] R. Kashyap. *Fiber Bragg Gratings* (Academic, N.Y., 1999).
[4] D. Kovalev, H. Heckler, G. Polisski, F. Koch. Phys. Status Solidi B, **215**, 871 (1999).
[5] S. Takeoka, M. Fujii, S. Hayashi, K. Yamamoto. Phys. Rev. B, **58**, 792 (1998).
[6] V.I. Klimov. J. Phys. Chem. B, **104**, 6112 (2000).
[7] H.-J. Fitting, T. Barfels, A.N. Trukhin, B. Schmidt, A. Gulans, A. von Czarnowski. J. Non-Cryst. Sol., **303**, 218 (2002).
[8] S. Agnello, R. Boscaino, M. Cannas, F.M. Gelardi, M. Leone, B. Boizot. Phys. Rev. B, **67**, 033 202 (2003).
[9] B. Schmidt. Report: *Preparation of* SiO_2:Ge *layers* (Research Center Rossendorf, 1997); *Preparation of* SiO_2:Si *and* SiO_2:O *layers* (Research Center Rossendorf, 2000).
[10] H.-J. Fitting, T. Barfels, A.N. Trukhin, B. Schmidt. J. Non-Cryst. Sol., **279**, 51 (2001).
[11] L. Rebohle, J. von Borany, H. Fröb, W. Skorupa. Appl. Phys. B, **71**, 131 (2000).
[12] A.N. Trukhin, H.-J. Fitting, T. Barfels, A. von Czarnowski. J. Non-Cryst. Sol., **260**, 132 (1999).
[13] H.-J. Fitting, T. Ziems, Roushdey Salh, M.V. Zamoryanskaya, K.V. Kolesnikova, B. Schmidt, A. von Czarnowski. J. Non-Cryst. Sol., **351**, 2251 (2005).
[14] M.A. Stevens Kalceff. Phys. Rev. B, **57**, 5674 (1998).
[15] E.V. Kolesnikova, A.A. Sitnikova, V.I. Sokolov, M. Zamoryanskaya. Sol. St. Phenomena, **108–109**, 729 (2005).
[16] L.A. Bakaleinikov, M.V. Zamoryanskaya, E.V. Kolesnikova, V.I. Sokolov, E.Yu. Flegontova. Phys. Sol. St., **46** (6), 1018 (2004).
[17] Roushdey Salh, A. von Czarnowski, M.V. Zamoryanskaya, K.V. Kolesnikova, H.-J. Fitting. Phys. Status Solidi A, **203**, 2049 (2006) / DOI 10.1002/pssa.200521443.
[18] K. Imakita, M. Fujii, Y. Yamaguchi, S. Hayashi. Phys. Rev. B, **71**, 115 440 (2005).
[19] S.M. Prokes, W.E. Carlos, S. Veprek, C. Ossadnik. Phys. Rev. B, **58**, 15 632 (1998).
[20] A.R. Wilkinson, R.G. Elliman. J. Appl. Phys., **96**, 4018 (2004).
[21] G. Ledoux, J. Gong, F. Huisken, O. Guillois, C. Reynaud. Appl. Phys. Lett., **80**, 4834 (2002).
[22] F. Iacona, G. Franzo, C. Spinella. J. Appl. Phys., **87**, 1295 (2000).
[23] M. Zacharias, J. Heitmann, R. Scholz, U. Kahler, M. Schmidt, J. Bläsing. Appl. Phys. Lett., **80**, 661 (2002).
[24] L.X. Yi, J. Heitmann, R. Scholz, M. Zacharias. J. Phys.: Condens. Matter, **15**, S2887 (2003).

Редактор Т.А. Полянская